Resource-Efficient Technologies 1 (2018) 47–54

TOMSK POLYTECHNIC UNIVERSITY

Resource-Efficient Technologies

journal homepage: http://ojs.tpu.ru/index.php/res-eff

Review article

ANALYSIS OF X-RAY WHISPERING GALLERY WAVES PROPAGATING ALONG LIQUID MENISCUSES

L.I. Goray[1],
lig@pcgrate.com

V.E. Asadchikov[2],
asad@ns.crys.ras.ru

B.S. Roshchin[2],
ross@crys.ras.ru

Yu.O. Volkov[2],
neko.crys@gmail.com

A.M. Tikhonov[3]
tikhonov@kapitza.ras.ru

[1]ITMO University,
49 Kronverkskiy Pr., St. Petersburg, Russian Federation, 197101

[2]A.V. Shubnikov Institute of Crystallography, RAS,
59 Leninskii Pr., Moscow, Russian Federation, 119333

[3]P. L. Kapitza Institute for Physical Problems, RAS,
2 Kosygina Str., Moscow, Russian Federation, 119334

Abstract

X-ray diffraction and fluorescence of whispering galleries (WGs) which propagate along meniscuses of deionized water or silica hydrosols enriched by CsOH have been analyzed for the first time. The measurements have been performed using the diffractometer with a moving tube-detector system. The X-ray beam rotation angle reached a maximum value of 4° on a silica hydrosol sample. The WG mode propagating near the surface of a concave meniscus as well as the fluorescence intensity have been found from a solution of the respective Helmholtz equations. For analysis of intensities of the X-ray scattering and fluorescence we have used a two-layer model of the liquid with the upper non-uniform corrugated layer in which the concentration of levitating Cs^+ ions near the surface has a maximum derived from the experiment in the hydrosol depth of ~ 15 nm for SiO_2 particle sizes of ~ 5…7 nm. In order to determine the fluorescence intensity we have used the approach based on a method of fundamental parameters using the reciprocity theorem.
Keywords: whispering gallery, concave liquid meniscus, levitating Cs^+ ions, X-ray reflectometry, X-ray fluorescence, Helmholtz equation, method of fundamental parameters, reciprocity theorem.

☆ Peer review under responsibility of Tomsk Polytechnic University.
https://doi.org/10.18799/24056537/2018/1/182

1. Introduction

Whispering gallery (WG) is one of the most interesting wave phenomena. It has been known from antique architectural acoustics and means wave propagation along curved surfaces with high intensities. The name reflects the fact that a wave in closed space sometimes propagates not along the shortest path but rather along concave walls or domes. The relevant physical effect, wave propagation along curved interfaces between two media, is known in other wave processes as well including electromagnetic wave propagation.

Extreme sensitivities of WG sensors not only lead to a breakthrough in biodetection but also enables sensitive probing of physical and micromechanical oscillator via optomechanical coupling and laser resonators. Many other sensor applications are also under active research and development in which different sensor geometries, materials, surface modifications and device integration strategies are explored. In X-rays, WGs can be very attractive for applications as beam splitters and beam rotators. In this work we analyze for the first time diffraction of X-ray WG waves which propagate along the large-radius meniscus of deionized water or silica hydrosols enriched by CsOH.

2. Experimental

The experiments have been performed on the "butterfly-type" diffractometer with the independently moving source-detector system [1]. All measurements have been conducted with the use of a laboratory X-ray tube at the radiation energy E = 8048.05 eV (Cu-Kα characteristic line, λ = 1.5405±0.0001 Å).

A concave surface meniscus has been formed by the controlled rotation of the round fluoroplastic trough (100 mm in diameter) which held the liquid sample (Fig. 1). The rotation regime, angular position of incident X-ray beam and height position of the sample trough have been calibrated with the use of de-ionized water as a sample which allowed us to rotate the incident beam by 1°. To increase the sample holder stability an additional vibration protection system has been installed.

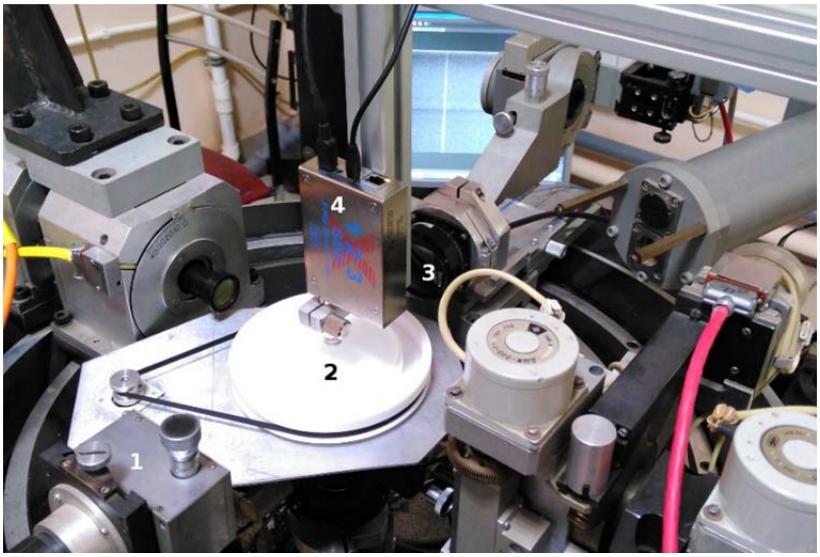

Fig. 1. A photograph of the laboratory X-ray diffractometer to measure WG modes in liquid meniscus:
1 – collimating slit system for incident beam, 2 – rotating fluoroplastic sample-holding trough, 3 – two-dimensional X-ray detector, 4 – X-ray fluorescence detector

Further measurements have been carried out using colloidal silica hydrosols as samples instead of de-ionized water. Characteristic diameters of SiO_2 particles in the hydrosols have been previously estimated in the range of 7…27 nm [2]. The advantages of the usage of the silica sols for the observation of WG effects are tied to their higher viscosity compared to clean water which leads to the lower sensibility to vibrations. Dielectric permittivity δ and absorption γ values calculated for H_2O and silica hydrosols doped by alkali ions are presented in Table 1.

Table 1. Calculated values of electron density and dielectric permittivity

matter	ρ_e, Å^{-3}	E = 8048 eV		E = 70967 eV	
		δ	γ	δ	γ
H_2O	0.3353	7.128×10^{-6}	2.390×10^{-8}	9.121×10^{-8}	1.648×10^{-11}
FM+NaOH	0.3639	7.737×10^{-6}	3.693×10^{-8}	9.892×10^{-8}	2.810×10^{-11}
FM+CsOH	0.3792	8.061×10^{-6}	7.932×10^{-8}	1.030×10^{-7}	8.331×10^{-11}
FM+RbOH	0.3762	7.997×10^{-6}	4.661×10^{-8}	1.023×10^{-7}	1.227×10^{-10}
SM+NaOH	0.3981	8.463×10^{-6}	5.124×10^{-8}	1.081×10^{-7}	4.081×10^{-11}
SM+CsOH	0.4164	8.853×10^{-6}	1.021×10^{-7}	1.131×10^{-7}	1.071×10^{-10}
TM+NaOH	0.4031	8.570×10^{-6}	5.458×10^{-8}	1.095×10^{-7}	4.384×10^{-11}
TM+CsOH	0.4159	8.841×10^{-6}	8.990×10^{-8}	1.129×10^{-7}	8.985×10^{-11}

The enrichment of a sample by CsOH allowed us to measure the fluorescence yield along the sample surface. The position of the maximum of the fluorescence yield was found to be shifted by 25 mm from the sample center to the X-ray source position and slowly decreased in the opposite position which corroborates the transmission of the X-ray beam along the surface. The estimated diameter of a meniscus area transmitting whispering gallery modes is ~ 50 mm, while the beam rotation angle achieved $\psi = 4°$ (Fig. 2).

Fig. 2. Two-dimensional images of the incident beam (left) and beam reflecting from a concave meniscus of silica hydrosol, rotated by the WG effect on 2° (center) and 4° (right)

3. Model

For qualitative analysis and comparing with the measurements of X-ray scattering and fluorescence intensities we have used a two-layer model of the liquid with the upper non-uniform corrugated layer. The two-layer model includes: (a) variations of the electron density profile (Fig. 3); (b) an air-liquid surface sine-shaped ripples with the Gaussian height distribution and the Gaussian correlation function. It has been found [2, 3] that alkali ions form a suspended layer on the surface of silica sol. In the case of an FM sol (SiO_2 particles having size ~ 7 nm) enriched by CsOH, the previously-found depth-distribution of electron density is presented in Fig. 3; the thickness of the Cs^+ ion layer at the surface is ~ 2.5 nm, while the estimated in-plane concentration of Cs^+ ions is ~ $4\cdot10^{18}$ m^{-2}. The derived concentration of levitating Cs^+ ions has a sharp maximum exactly at the sol's surface. In addition, there is a broad maximum in particles concentration in the hydrosol depth of ~ 15 nm.

3.1. Reflectometry

We have used a quasi-grating model due to the surface waves and near-zone ripple ordering including: thermal capillary waves [4] and quasi-periodical surface clusters [5]. In the model we have used under ripples a number of very thin uniform rectangular layers, the so-called staircase approximation. The layer was divided by 32 uniform thin layers with the total layer depth $H = 57.7$ nm. The average size of ripples $\langle h \rangle = 3$ nm and their correlation length $\zeta \sim 100$ nm were derived by our atomic-force microscopy (AFM) measurements of surfaces of silica hydrosols and also by the measurements of two-dimensional clusters of polypeptide molecules [6].

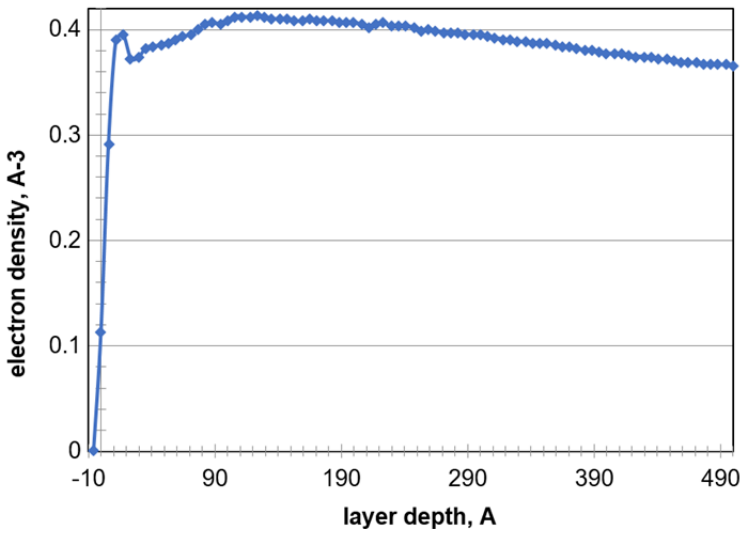

Fig. 3. Volume electron density distribution inside the upper non-uniform layer of hydrosol Ludox FM + CsOH

The WG mode structure near the surface of a concave meniscus can be found from a solution of the respective Helmholtz (or parabolic as an approximation) equation. Asymptotics of such glancing incidence waves are mostly determined by behaviour of Airy functions near the zeros (e. g., in [7]). In cases of small roughness (rms about a few nm) and big enough meniscus radiuses ($r \gtrsim 10$ cm), X-ray radiation losses can be ignored [8]. Then, the reflectance accounting quadratic terms on the grazing incidence angle θ that may be important in considered cases is determined for the rotating angle ψ as

$$R(\theta, r, \psi) = I_0(\theta, r, 0)\exp\{-2\psi Re\left[\frac{\eta}{\sqrt{\varepsilon-1}} - \frac{\theta\eta^2}{\varepsilon-1}\right]\}, \quad (1)$$

where $I_0(\theta, r, 0)$ is an incident intensity, $\eta = 1$ or $\eta = \varepsilon$ for TE or TM polarizations, respectively, and $\varepsilon = 1 - \delta + i\gamma$ is the matter permittivity. For a low-absorbing regime $\gamma << \delta$ and closely to the 0-angle incidence, it can be calculated using the well-known expression:

$$R(\theta, r, \psi) = I_0(\theta, r, 0)\exp\{-2\psi Re\left[\frac{\eta}{\sqrt{\varepsilon-1}}\right]\}. \quad (2)$$

As predicted by the capillary-wave model, the roughness of interfaces is higher for liquids with smaller surface tensions, i. e. easier to excite thermal roughness on surfaces with smaller stiffness. Silica hydrosols have higher surface tensions and higher stiffness in comparison with such parameters for H_2O. The experimental value for the surface tension of the hydrosol's surface is ~ 74 mN/m that is slightly higher than for the water's surface (72.5 mN/m). Indeed, the hydrosol surface is very clean since its bulk is a very strong adsorbent. Hydrosols have also the smaller fractal surface roughness connected with vibrations of the step motor which rotates the cup with liquids. The higher viscosity of a liquid is, the smaller fractal roughness is. In the good approximation, one can use for the effective roughness σ_{eff}

$$\sigma^2_{eff} = \sigma^2_{capil} + \sigma^2_{fract}. \quad (3)$$

It is known from measurements [5, 6] that for plane H_2O surfaces the rms roughness due to capillary waves is ~ 0.3 nm. For concave rotating meniscuses, as it will be demonstrated further by our scattering intensity calculus, σ_{eff} (H_2O) is $\gtrsim 5$ nm, σ_{eff} (Ludox FM) is ~ 1.5 nm.

To determine the scattering intensity we have used numerical calculations based on the rigorous method of boundary integral equations developed, in particular, to analyze X-ray gratings and randomly-rough multilayer mirrors [9]. To compute the model, we have used PCGrates commercial software [10]. The rigorous approach

allows one to account exactly the electron density (refractive index) varying in the upper non-uniform layer with sine ripples, absorption and polarization. In Fig. 4 the specular reflectance of the silicon hydrosol (Ludox FM) with levitating near the surface Cs+ ions are calculated by various absorption models.

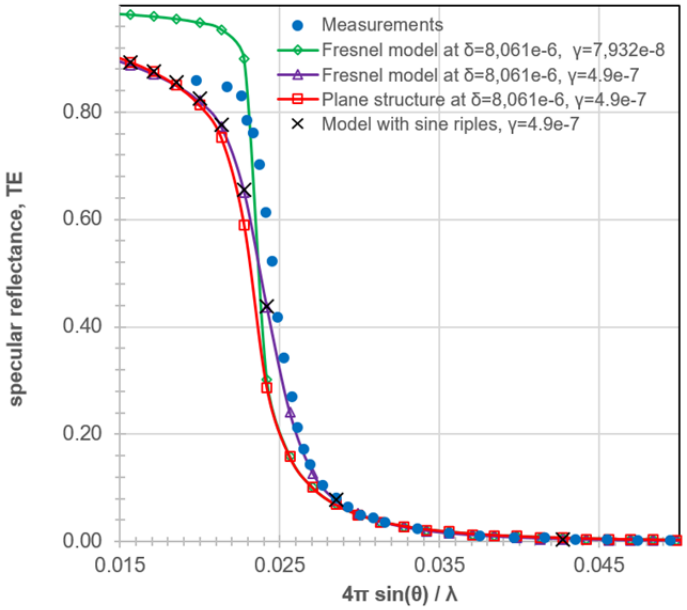

Fig. 4. Specular reflectance of silica hydrosol with Cs^+ ions for different absorption models

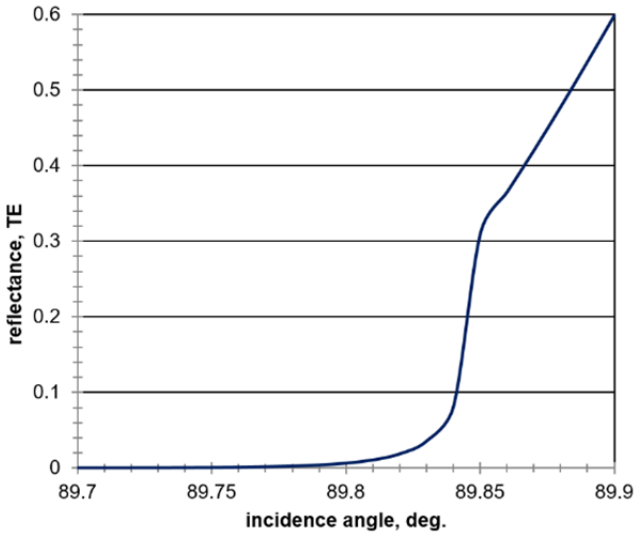

Fig. 5. Specular reflectance of the WG mode on H_2O for ψ = 1° (4 reflections) and σ_{eff} = 5 nm in the Debye-Waller roughness model

As one can see in Fig. 5, the specular reflectance peak of WG modes propagating along the concave H_2O surface is destroyed almost totally, even for a 1-degree rotation (4 reflections), due to high depth ripples (σ_{eff} = 5 nm in the Debye-Waller roughness model). Such behavior is in good agreement with the reflectance measurements (Fig. 2 and 4) and due to the motor vibration and low viscosity. In contrast to the H_2O surface, the reflectance of WG modes propagating near a Ludox FM surface is high (σ_{eff} = 1.5 nm in the rigorous model accounting roughness [9]), even for a 4-degree rotation (14 reflections). The experimental data obtained (bold markers) match perfectly the theoretical curves (Fig. 6) calculated for the above mentioned complex model with sine ripples and for the grazing incidence angle of ~ 0.16°.

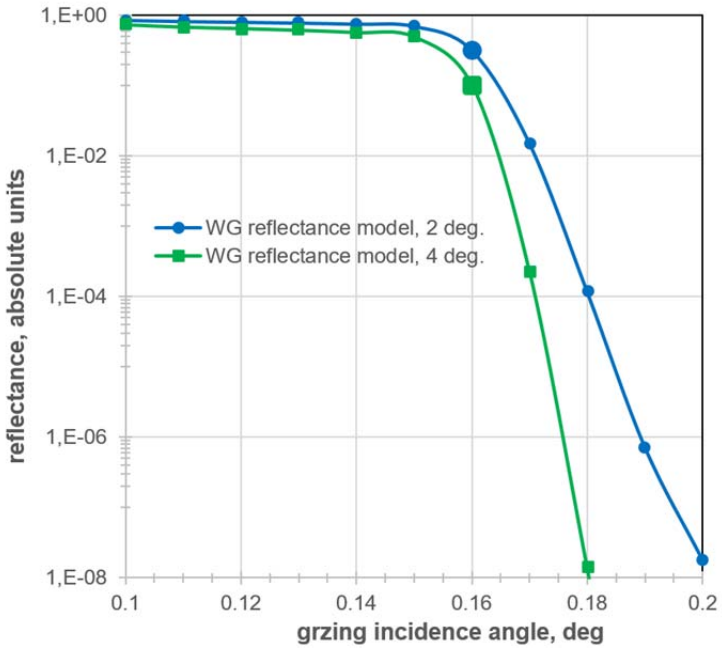

Fig. 6. Specular reflectance for the model with the upper non-uniform layer and sine ripples: for a 2-deg rotation (blue) and for a 4-deg rotation (green)

3.2. Fluorescence

To determine the fluorescence intensity we have used the numerical approach on the basis of a method of fundamental parameters. The method of fundamental parameters is based, basically, not on the use of an external or internal standard, but on the application of direct calculation (performed in some way) of the intensity of the X-ray fluorescence line [11]. In the general approach under consideration, the concentration of the unknown element c is determined from the known concentration of the same element in the reference sample c_0 and the intensity of the primary radiation in the known sample I'_0 from a relationship in the form

$$c = c_0 (I' / I'_0) (I_0 / I), \tag{4}$$

where a suitable expression for the intensity of the X-ray fluorescence line I in an unknown sample is used in an explicit form containing such fundamental parameters as mass absorption coefficients, absorption edges, fluorescence yields and others.

Expression (4) is based on the assumption that the intensity of secondary radiation obtained from a certain depth from the chemical element of a certain concentration is proportional to the square of the strength (in the dipole approximation) of the electric field (its intensity) and the concentration of this element. A fluorescence analysis scheme with the primary radiation of an X-ray tube incident at an angle φ_1 relative to the sample surface and an analyzer detector located at an angle φ_2 is shown in Fig. 7. The secondary X-ray radiation is registered from a layer of thickness dx at a depth of x. As shown by numerous experimental and theoretical studies, this assumption is valid in a wide range of the parameters considered. The intensity of the incident radiation at some boundary of the multilayer sample can be accurately determined by solving Maxwell's equations (or the vector Helmholtz equation). For a conventional multilayer with perfect flat interfaces, this solution is Parratt's recurrence formulae. However, for structured interfaces the task is much more complicated and can be solved exactly, in general, only by using time-consuming numerical calculations [9]. The most difficult is to express the dependence $I(c)$ explicitly in terms of the fundamental and gauge (normalization) parameters and, thus, solve (4). Various methods of fundamental parameters imply different approaches for finding I.

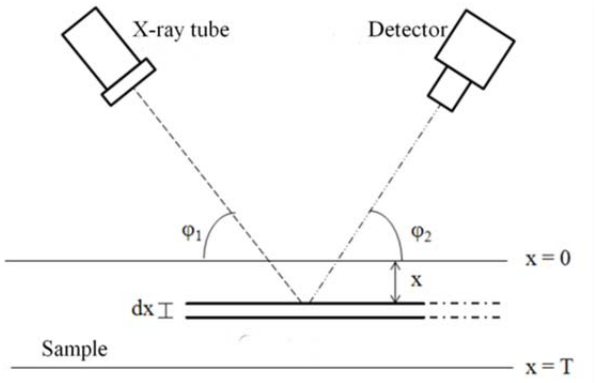

Fig. 7. A fluorescence analysis scheme.

A theoretical approach similar to ours was first applied in [12] to analyze the intensity of X-ray fluorescence on a multilayer stack with perfect plane boundaries. The main stages of this approach are as follows. In the first step, the intensity of the exciting electromagnetic field equal to $|E_{ex}(\varphi_1, x)|^2$ is calculated for a given incidence angle φ_1 and the penetration depth into sample x (Fig. 7). As already noted, in the case of flat interfaces this can be done easily with the help of Parratt's recurrence formulas or any matrix formalism. In the case of structured (corrugated) interfaces, it is required to solve numerically the two-dimensional or three-dimensional Helmholtz equation with the rigorous boundary conditions and radiation conditions. Then the fluorescence intensity obtained at the depth of sample x is proportional to the intensity of the exciting field and the concentration of the unknown element $c(x)$:

$$|E_{fl}(\varphi_1, x)|^2 = a\, c(x)\, |E_{ex}(\varphi_1, x)|^2, \tag{5}$$

where a is a certain proportionality coefficient.

Further it is necessary to calculate the fluorescence intensity value $|E_{fl}(\varphi_2, x)|^2$ arriving at the detector at the grazing incidence angle φ_2 from a source located at a depth of x. We use the reciprocity theorem which states that the electromagnetic field produced by the dipole source on a detector is identical to the field created at the source site by an analogous dipole located at the site of the detector. Taking into account that the distance from the source to the detector is much larger than the thickness of the layer under investigation, the quantity $|E_{fl}(\varphi_2, x)|^2$ can be calculated using the same formalism as for $|E_{ex}(\varphi_1, x)|^2$ under the assumption that the fictitious source is at infinity in the direction of detection.

Finally, the intensity of the characteristic fluorescent radiation is determined by the product:

$$|E_{fl}(\varphi_1, \varphi_2, x)|^2 = q\, c(x)\, |E_{ex}(\varphi_1, x)|^2\ |E_{fl}(\varphi_2, x)|^2, \quad (6)$$

where q is a certain proportionality coefficient. Thus, the concentration of an unknown element or substance (its mass volume) can be found using (6) when solving the inverse problem of X-ray fluorescence.

It should be noted that this method makes it possible to calculate the fluorescence intensity equally accurately in both the direct and reciprocity schemes. This imposes an additional constraint on the adjustable parameter q which should provide a better fit simultaneously for both schemes. In the proposed approach, among the fundamental parameters under consideration, it is especially important to distinguish the matrix mass attenuation coefficient given by the composition of the analyzed multilayer structure, and also the effective photoelectron absorption cross section, which determine the effect (probability) of fluorescence itself. Also, an influence of the geometrical factor to fluorescence intensity yields should be accounted, i. e. a part of the concave liquid surface where a number of converging WG rays is maximal.

The linear absorption coefficient which appears as the product of the mass coefficient of attenuation by the density ($\mu\rho$) is related to the photoabsorption cross section determined by the imaginary part of the atomic scattering factor. This universal relationship for any substance and interface is given by a simple expression:

$$\mu\rho = 4\pi A/\lambda, \quad (7)$$

where A is the dimensionless absorption coefficient computed in the explicit form (in quadratures) in the program on the basis of the rigorous solution for near-zone fields of Maxwell's equations. This coefficient which characterizes Joule's energy losses in matter as well as magnitudes of the electromagnetic field and their derivatives can be independently calculated in the code at any depth of the sample (on any real or fictitious boundary). In addition to the physical meaning, A is a measure of the accuracy and convergence of calculation results performed in one iteration, as it enters the energy balance of a grating [9]. This balance in the case under consideration will be determined not only by the losses due to Rayleigh's scattering and the resistive absorption but also by the total power of detected fluorescence line.

4. Conclusion

We consider theoretically and experimentally diffraction of X-ray whispering gallery waves which propagate along large-radius meniscuses of deionized water or silica hydrosols. An exit of grazing incidence X-ray fluorescence of ions Cs^+ levitating near the hydrosol surface has been demonstrated and tested. Our numerical results are compared qualitatively and quantitatively with those obtained using the fulfilled experiments and simple analytical technique. In the model of finding scattering and fluorescence intensities of the glancing X-ray radiation, the roughness and diffuseness of interfaces along with thicknesses and electron densities of layers are not fitting but taken from measurements or respective computations and incorporated into the rigorous solution of Maxwell's equations that is another advantage of the proposed approach.

Acknowledgements

This work was partially supported by the Ministry of Education and Science of the Russian Federation and the Russian Foundation for Basic Research (17-02-00362, 16-29-11697).

Conflict of interest

The authors declare no conflict of interest.

References

[1] Asadchikov V.E., Babak V.G., Buzmakov A.V. et. al. An X-ray diffractometer with a mobile emitter-detector system. *Instruments and Experimental Techniques,* 2005, vol. 48, no. 3, pp. 364–372. DOI: 10.1007/s10786-005-0064-4.

[2] Asadchikov V.E., Volkov V.V., Volkov Yu.O. et. al. Condensation of silica nanoparticles on a phospholipid membrane, *Journal of Experimental and Theoretical Physics Letters*, 2011, vol. 94, no. 7, pp. 585–587. DOI: 10.1134/S002136401.

[3] Tikhonov A.M. Compact Layer of Alkali Ions at the Surface of Colloidal Silica, *J. Phys. Chem. C*, 2007, vol. 11, no. 2, pp. 930–937. DOI: 10.1021/jp065538r.

[4] Ocko B.M. X-Ray Reflectivity and Surface Roughness. In: *Spectroscopic and Diffraction Techniques in Interfacial Electrochemistry*, C. Gutiérrez, C. Melendres, eds. NATO ASI Series, 1990. DOI: 10.1007/978-94-011-3782-9.

[5] Fukuto M., Heilmann R.K., Pershan P.S. et al. X-Ray Measurements of Noncapillary Spatial Fluctuations from a Liquid Surface, Phys. Rev. Let., 1998, vol. 81, p. 3455. DOI: 10.1103/PhysRevLett.81.3455.

[6] Pershan P.S.. Effects of thermal roughness on X-ray studies of liquid surfaces. *Colloids and Surfaces A*, 2000, vol. 171, no. 1–3, pp. 149 –157. DOI: 10.1016/S0927-7757(99)00557-9.

[7] Babich V.M., Buldyrev V.S.. *Asymptotic Methods in Short-Wavelength Diffraction Theory*. Alpha Science International Limited, Oxford, 2007, 480 p.

[8] Bukreeva I.N., Kozhevnikov I.V., Vinogradov A.V. *Journal of X-ray Science and Technology*, 1995, vol. 5, no. 4, pp. 397–419. DOI: 10.1016/S0895-3996(85)80005-7.

[9] Goray L.I., Schmidt G. Boundary Integral Equation Methods for Conical Diffraction and Short Waves. In *Gratings: Theory and Numerical Applications*., E. Popov, ed., 2nd rev. ed. Presses Universitaires de Provence, AMU, 2014, pp. 447–536.
Website of International Intellectual Group, Inc. URL: http://www.pcgrate.com/.

[10] He F., Van Espen P.J. General Approach for Quantitative Energy Dispersive X-ray Fluorescence Analysis Based on Fundamental Parameters. *Analytical Chemistry*, 1991, vol. 63, no. 20, pp. 2237–2244. DOI: 10.1021/ac00020a009.

[11] Chauvineau J.-P., Bridou F. Analyse angulaire de la fluorescence du fer dans une multicouche périodique Fe/C, 1996, *J. Physique IV*, vol. 06, no. C7, pp. 53–64. DOI: 10.1051/jp4:1996707.